A New Look at Solar Irradiance Variation

Peter Foukal

Solar Physics

279/1

Springer

ISSN 0038-0938

Springer

Springer

A New Look at Solar Irradiance Variation

Peter Foukal

Abstract We compare total solar irradiance (TSI) and ultraviolet (F_{uv}) irradiance variation reconstructed using Ca K facular areas since 1915, with previous values based on less direct proxies. Our annual means for 1925–1945 reach values 30–50 % higher than those presently used in IPCC climate studies. A high facula/sunspot area ratio in spot cycles 16 and 17 seems to be responsible. New evidence from solar photometry increases the likelihood of greater *seventeenth century* solar dimming than expected from the disappearance of magnetic active regions alone. But the large additional brightening in the *early twentieth century* claimed from some recent models requires complete disappearance of the magnetic network. The network is clearly visible in Ca K spectroheliograms obtained since the 1890s, so these models cannot be correct. Changes in photospheric effective temperature invoked in other models would be powerfully damped by the thermal inertia of the convection zone. Thus, there is presently no support for twentieth century irradiance variation besides that arising from active regions. The mid-twentieth century irradiance peak arising from these active regions extends *20 years* beyond the early 1940s peak in global temperature. This failure of correlation, together with the low amplitude of TSI variation and the relatively weak effect of Fuv driving on tropospheric *temperature*, limits the role of solar irradiance variation in twentieth century global warming.

Keywords Solar activity · Solar irradiance

1. Introduction

Reconstructions of past radiative inputs to climate continue to improve through advances in understanding of solar irradiance variation (see reviews and discussions by, *e.g.*, Foukal *et al.*, 2006; Krivova and Solanki, 2008; Fröhlich, 2011). Until recently, for instance, no measurement of the facular area variation which dominates the 11-year (yr) irradiance modulation (Foukal and Lean, 1988; Lean, 1987) was available prior to the past few solar cycles.

P. Foukal (✉)
Heliophysics Inc., 192 Willow Rd., Nahant, MA 01908, USA
e-mail: pvfoukal@comcast.net

Digitizations of the Mt. Wilson, Sacramento Peak, Kodaikanal, and other shorter Ca K spectroheliogram archives now provide area measurements of faculae in both active regions and active networks extending back to 1907 (Foukal, 1996, 1998a, 1998b, 2002; Foukal *et al.*, 2009; Tlatov, Pevtsov, and Singh, 2009; Bertello, Ulrich, and Boyden, 2010; Ermolli *et al.*, 2009). In Section 3 we discuss how these new data improve our understanding of the 11-yr irradiance variation.

Tropospheric temperature response to 11-yr total solar irradiance (TSI) variation has been reported (*e.g.*, North, Wu, and Stevens, 2004; Camp and Tung, 2007). Temperature forcing by ultraviolet flux (F_{uv}) variation seems less effective unless additional couplings are included (Meehl *et al.*, 2009). Reconstructions of the changing amplitude of the 11-yr irradiance variation provide the impetus for the climate models used by the Intergovernmental Panel on Climate Change (IPCC) (Solomon *et al.*, 2007). It is now generally accepted that centennial-scale modulation of 11-yr TSI driving alone is too small to explain the global warming reported since the seventeenth century (*e.g.*, Wigley and Raper, 1990). Volcanism may have caused much of this seventeenth century cooling (*e.g.*, Crowley, 2000). But one cannot rule out some driving of the subsequent warming by a larger TSI increase than could be caused by spots and faculae alone.

Several arguments for such larger TSI variations have appeared (*e.g.*, Lean, Skumanich, and White, 1992; Lockwood, Stamper, and Wild, 1999; Tapping *et al.*, 2007; Steinhilber, Beer, and Fröhlich, 2009; Shapiro *et al.*, 2011). There is less motivation to seek slow variations of F_{uv} larger than its measured 11-yr amplitude, since that amplitude is already sufficient to drive the changes in tropospheric circulation and precipitation that seem to constitute the main climate effects of this "top-down" mechanism (*e.g.*, Haigh, 1996; Haigh, Blackburn, and Day, 2005; Shindell *et al.*, 2006).

In Section 4 we review new evidence for greater solar dimming during *extended* periods of lower activity, such as occurred during the seventeenth century Maunder Minimum. But we point out in Sections 4 and 5 that models which claim climatically significant solar brightening during the twentieth century either contradict observational evidence or overlook basic physical properties of the Sun. These contradictions cast doubt on the validity of these models when also applied to earlier centuries and millennia.

2. A Simple Model of Irradiance Variation

2.1. Variation of TSI

We construct the most straightforward model of TSI variation that i) reproduces the spaceborne radiometry to within measurement errors, and ii) can be extended back to the beginning of the sunspot record in the early seventeenth century. We focus on annual means, rather than shorter time scales, since our interest is in variations considered most likely to drive climate on multi-decadal and longer time scales.

The only suitable approach to achieve these two aims is through regression of TSI (after correction for sunspot blocking) against a full disk index of the TSI contribution of faculae in both active regions and the enhanced network (Foukal and Lean, 1988). Our TSI values are taken from the Physico-Meteorological Observatory of Davos (PMOD) composite (Fröhlich, 2009). We use values after 1980, when the first measurements from the Active Cavity Radiometer Irradiance Monitor (ACRIM) became available (Willson *et al.*, 1981). We adopt an (annual mean) zero value of TSI = 1365.5 W m^{-2}, recorded during the solar minimum in 1986, as representative of the average quiet Sun. Recalibration of the TSI scale

has been proposed by Kopp and Lean Kopp and Lean (2011); we retain the earlier value here until remaining uncertainties in pyrheliometer characterization are resolved.

We chose the three most complete facular indices, moving backward in time. These are i) the A_{pn} series of projected facular areas obtained from the Mt. Wilson (MWO) and Sacramento Peak (SPO) archival images between 1916 – 1999 in the Ca K line (Foukal, 2002). The annual means of A_{pn} agree closely with two independent reductions of the MWO facular areas (Foukal *et al.*, 2009; Tlatov, Pevtsov, and Singh, 2009; Bertello, Ulrich, and Boyden, 2010). (See also Figure 8 in the Appendix.) The Kodaikanal (KKL) Ca K index (Tlatov, Pevtsov, and Singh, 2009) is also briefly considered here, but its behavior requires further investigation (see the Appendix). We also use ii) the F10.7 microwave index, available since 1947, and iii) the sunspot and group numbers, R_Z, and R_g.

Of these four indices, only A_{pn} directly measures the facular area changes that cause the irradiance variation. The F10.7 index measures the 10.7 cm microwave flux that arises mainly from thermal free- free emission above these structures, with a smaller contribution from gyro radiation above sunspots (Tapping, 1987). Its density and field intensity dependences somewhat complicate its use as a proxy of facular area variation; on the other hand, its microwave radiometric calibration offers the highest measurement accuracy. R_Z and R_g offer by far the longest time coverage, extending to the seventeenth century, although they are rather arbitrary solar activity indices (Hoyt and Schatten, 1998) whose variation is only loosely connected to facular area.

We construct a simple sunspot blocking function, P_s, from the formula: $P_s = (C_s - 1)A_s = 0.33A_s$. Here, C_s is the mean, broadband, photometric contrast of a spot, averaged over umbra and penumbra. Reported dependences of C_s on spot size and cycle phase are neglected here; their effect falls within uncertainties in the radiometry and area measurements. A_s is the series of annual mean projected, total (umbral + penumbral) areas measured in millionths of the solar disk. We used the Royal Greenwich Observatory (RGO) annual values available between 1875 – 1976 as given by the National Geophysical Data Service (NGDC), extended beyond 1976 by D. Hathaway.

2.2. Variation of F_{uv}

The photochemistry of ozone is determined almost entirely by solar UV radiation between about 130 – 240 nm; longer wavelengths have negligible influence (*e.g.*, Foukal, Chulsky, and Weisenstein, 2008). Thus our reconstruction of variation in ultraviolet flux, F_{uv}, applies to this ozone-effective wavelength range. The brightness contrast of faculae increases with decreasing wavelength through the visible and UV spectral regions (*e.g.*, Chapman and McGuire, 1977). Below about 250 nm the contribution of spots to F_{uv} variation becomes negligible (Lean, 1987), and its fractional variability is dominated simply by variations in facular projected area. That is, $\Delta F_{uv}/F_{uv} = C(\lambda)A_{pn}$, where $C(\lambda)$ expresses the disk-averaged brightness contrast of faculae at wavelength λ, and A_{pn} is expressed as fractional coverage of the solar disk. If we are interested only in the *time behavior* of F_{uv} variation (*i.e.*, not in the magnitude of its variation), we can ignore the contrast values, $C(\lambda)$, and simply study the time series of A_{pn}.

3. Results

3.1. Modeling the Space-Borne TSI Radiometry between 1980 – 1999

In Figure 1 we compare TSI reconstructions using the three facular indices. The radiometry is shown along with the TSI reconstructed from F10.7 and R_Z in panel (a) and from two
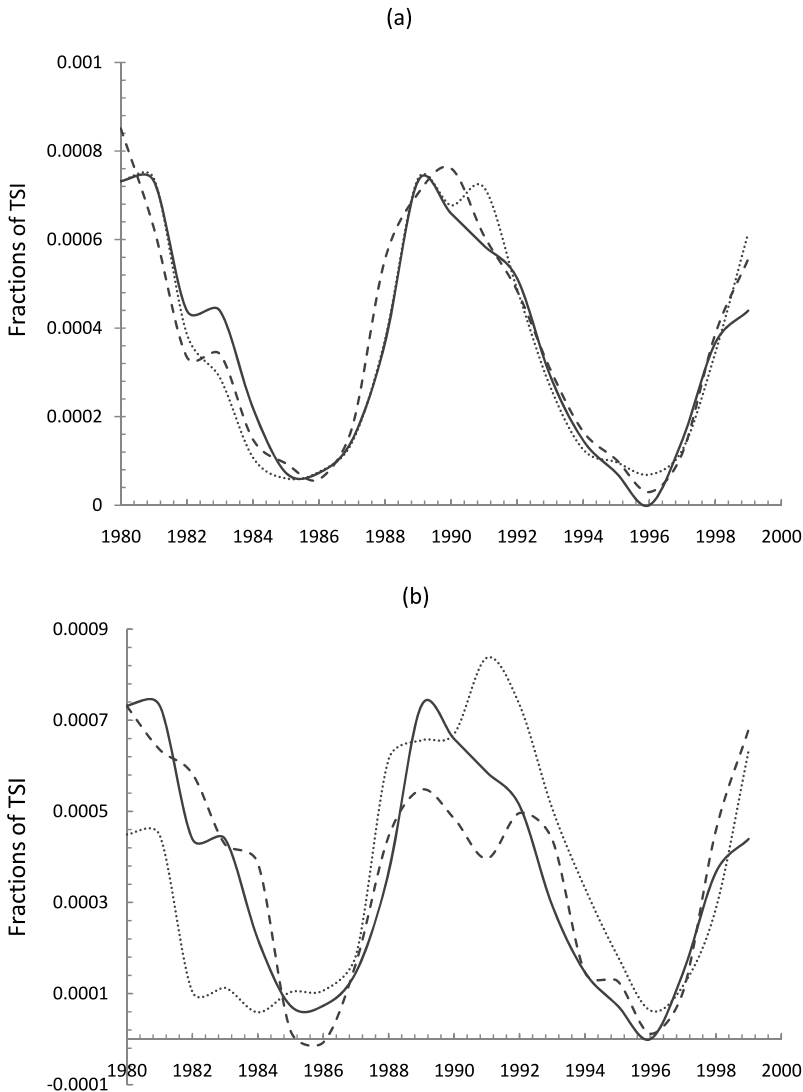
(a)

(b)

Figure 1 Panel (a): Radiometry (solid), TSI reconstructed from F10.7 (dotted) and from R_Z (dashed), for 1980 – 1999. Panel (b): Radiometry (solid) and TSI from SPO facular areas (Tlatov, Pevtsov, and Singh, 2009) (dashed), and from A_{pn} (dotted).

Ca K indices in panel (b). The Ca K data for A_{pn} are available only to 1999, so we can carry our reconstructions only to that date.

   The correlation obtained using the Ca K measures is noticeably less good (correlation coefficient $r \approx 0.7 - 0.88$) than that obtained using either F10.7 or R_Z ($r \approx 0.95$). These results are insensitive to the choice of P_s; similar results are obtained using a P_s series provided by C. Fröhlich (approximately the same as ours multiplied by 0.81). The results also change little if the regressions of the radiometry against F10.7 and R_Z used for these reconstructions are based on the period 1980 – 1989 or the longer period 1980 – 2009.
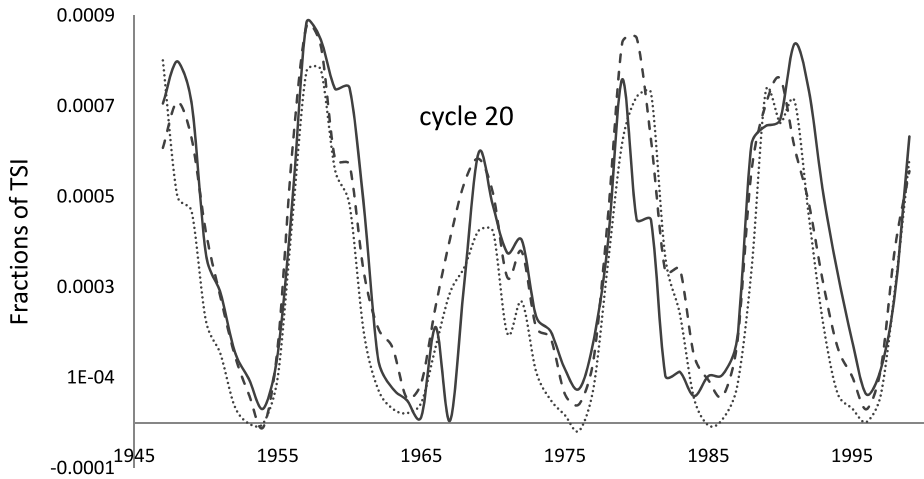
Figure 2 TSI (A_{pn}) (solid), TSI (R_Z) (dashed), and TSI (F10.7) (dotted), all for 1947 – 1999.

The most likely explanation is uncertainty in the Ca K areas for this specific period when reliable space-borne TSI measurements are available. Most of this period occurs after the end of the MWO Ca K spectroheliogram series in 1984. Agreement between three independent reductions of the 1915 – 1984 MWO data is remarkably good, as mentioned in Section 2. However, agreement is less good on the relative amplitudes of cycles 21, 22 between the two independent reductions by Foukal (2002) and by Tlatov, Pevtsov, and Singh (2009) of the SPO Ca K spectroheliograms for 1985 – 1999. This weaker agreement is reflected in the difference of the dotted and dashed TSI curves in Figure 1(b).

3.2. TSI between 1947 – 2009

In Figure 2 we compare the three TSI reconstructions using A_{pn}, R_Z, and F10.7 for the period 1947 to 1999. The F10.7-based TSI reconstruction, TSI (F10.7), lies about 30 % below the A_{pn} and R_Z-based reconstructions in cycle 20. This is caused partly by TSI (F10.7) reaching values closer to zero at the 1976 and 1986 minima. We expect the F10.7-based reconstruction to be more reliable at the minima, when percentage errors in R_Z and especially in A_{pn} become most significant. We have seen that TSI (F10.7) correlates with the radiometry over 1980 – 1999 as well or better than TSI (R_Z), so this advantage in zero point accuracy leads us to adopt it to represent TSI for the entire 1947 – 2009 period.

3.3. TSI between 1916 – 1946

In Figure 3 we compare the extension of the two A_{pn} and R_Z-based TSI time series, TSI (A_{pn}) and TSI (R_Z), back to 1916, when reliable annual means of A_{pn} began. The agreement between the two reconstructions is generally within ± 5 % with the exception of cycles 16 and 17. During those two cycles, spanning approximately 1925 – 1945, the TSI (A_{pn}) peaks reach values 30 – 50 % greater than those of TSI (R_Z).

Part of the difference is caused by a marked upward trend in the minima of TSI (A_{pn}) around 1933 and 1943 which is not present in the TSI (R_Z) time series. However, the amplitudes of the two cycles are also greater in TSI (A_{pn}), even after this trend is taken into
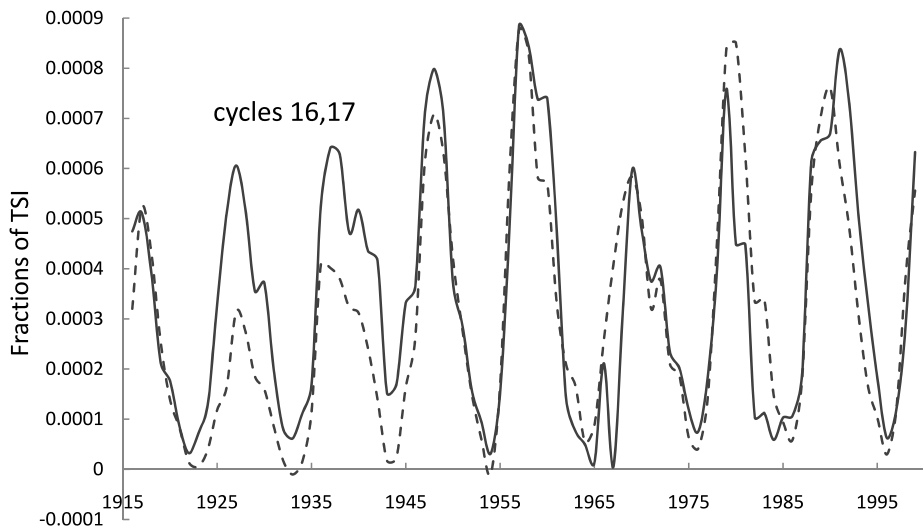
Figure 3 TSI (A_{pn}) (solid) and TSI (R_Z) (dashed) for 1916 – 1999.

account. An explanation must consider that the scales based on these same indices agreed in cycle 15, changed for cycles 16, 17, and then returned to agreement again for the cycles after 1946.

The 1926 – 1945 period corresponded to directorship of W. Brunner at the Observatory of the Federal Institute of Technology in Zurich. Svalgaard and Bertello (2009) report a 20 % increase in the scale of R_Z due to a personnel change in Zurich in 1946, when directorship was assumed by M. Waldmeier. This change is in the correct sense to explain the difference in TSI that we find. However, Svalgaard and Bertello (2009) find no evidence for a scale change at the beginning of Brunner's directorship in 1926.

The curve of TSI (R_Z) shown in Figure 3 is essentially the same as one of the two TSI forcings used in the most recent IPCC attribution studies of climate (Solomon *et al.*, 2007). Both are taken from Wang, Lean, and Sheeley (2005). In one, the facular contribution is represented by the sunspot group number, R_g, which is derived independently of R_Z (Hoyt and Schatten, 1998); thus, the difference between TSI (A_{pn}) and TSI (R_Z) is unlikely to be caused by a scale change in R_Z, which should not appear in R_g. An error in A_{pn} is also an unlikely explanation, given the agreement with facular areas measured independently by Bertello, Ulrich, and Boyden (2010) (see Figure 8 in the Appendix). The difference is most likely caused by real changes in the ratio of facular/spot areas for those cycles as reported earlier (Foukal, 1998b). Such cycle-to-cycle changes are an interesting feature of solar dynamo behavior (Brown and Evans, 1980; Foukal, 1998a).

The second IPCC forcing function contains a small uptrend in the TSI measured around activity minima. This trend is calculated by Wang, Lean, and Sheeley (2005) from a diffusion model of photospheric fields. This model has, in the past, illuminated some puzzling aspects of photospheric field rotation and relaxation (*e.g.*, Wang, Nash, and Sheeley, 1989). But its use to generate TSI trends from the enhanced network carried over between cycles is less well founded. The large observed cycle-to-cycle variations in facula/spot area ratio that cause the higher TSI values in cycles 16 and 17 are *not* the result of photospheric field diffusion. We know this because these ratio variations are observed already in the first year

of a cycle when active regions are very few, so diffusive cancellation of fields between them is negligible.

For this and other reasons explained by Foukal (1998b), the main source of ratio variations seems to be cycle-to-cycle changes in the spatial spectrum of the fields produced by subphotospheric dynamo processes. These would appear as changes in the field *source function* in the model of Wang, Lean, and Sheeley (2005). Source function changes are not taken into account in the TSI calculations of Wang, Lean, and Sheeley (2005) (nor in related modeling by Solanki, Schüssler, and Fligge (2002)). Thus the trend in the second IPCC TSI function is questionable.

3.4. TSI and F_{uv} Variation since 1610

For completeness we extend our TSI reconstruction prior to 1916 to the beginning of sunspot records in 1610, following an approach similar to that used in several previous studies (*e.g.*, Foukal and Lean, 1990; Lean, Beer, and Bradley, 1995). Between 1875 and 1916, A_s remains available from the RGO data. But now R_Z instead of A_{pn} must be used as a (less certain) proxy of the facular contribution.

Prior to 1875, only R_Z (or the group number, R_g) remains to represent TSI. The accuracy of this approximation can be gauged from Figure 4, where the curve of TSI is now simply R_Z scaled to the radiometry between 1980–1999. Its agreement over the period 1875–1916 with the series TSI (R_Z) that includes spot blocking illustrates how well R_Z alone estimates TSI.

Given the changes in the relation between R_Z and A_{pn} noted above in cycles 16 and 17 and especially the decrease in accuracy of the spot statistics prior to the mid-nineteenth century (Hoyt and Schatten, 1998; Hathaway, Wilson, and Reichmann, 2002) omission of spot blocking probably does not significantly decrease the accuracy of TSI reconstruction *in this epoch*. Prior to 1874 we replace R_Z with the group number, R_g, as a more frequently sampled activity index (Hoyt and Schatten, 1998). Our reconstruction of annual mean TSI between 1610–2009 is shown in panel (a) of Figure 5. Values after 1980 are taken from the PMOD composite.
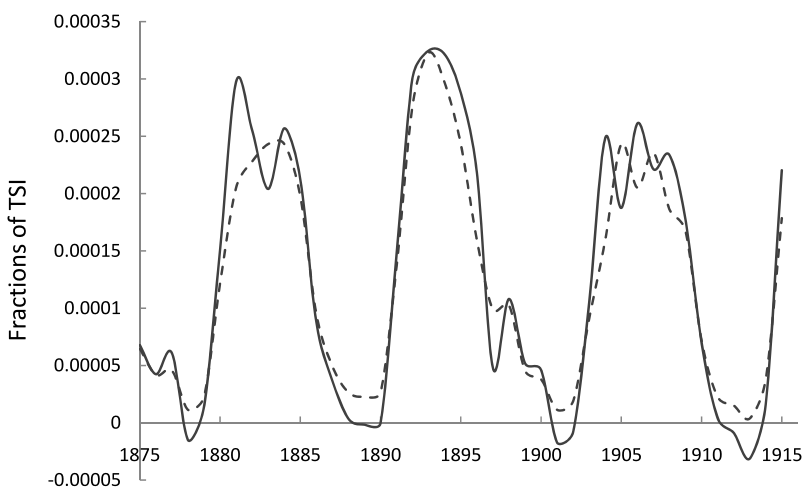

Figure 4 Comparison of TSI (R_Z) (solid) versus scaled R_Z alone (dashed), as alternative representations of TSI.

(a) TSI variation 1610 - 2009

Fractional variation
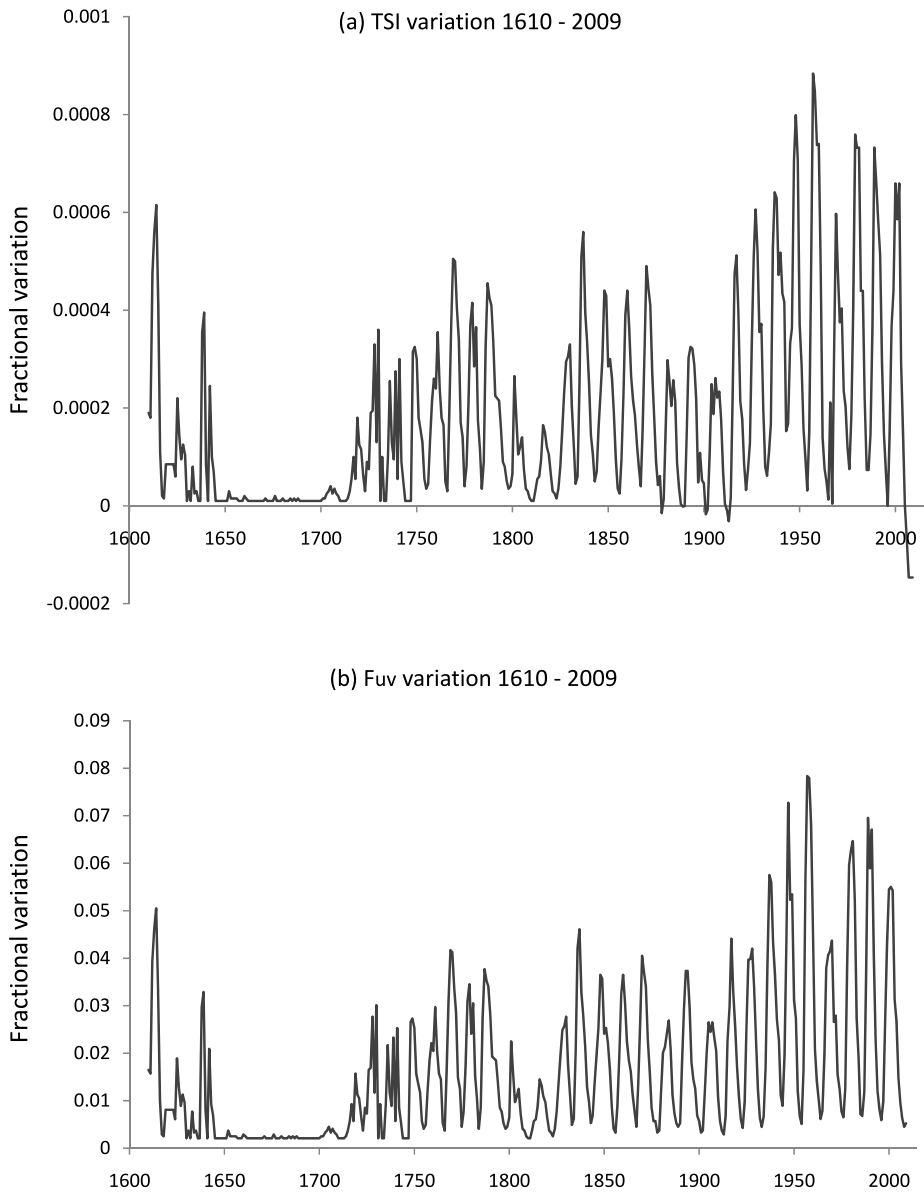
(b) Fuv variation 1610 - 2009

Fractional variation

Figure 5 (a) TSI composite and (b) F_{uv} composite in the period $1610-2009$. The ordinates are: (a) fractional variation of TSI; (b) fractional variation/$C(\lambda)$, where $C(\lambda)$ is the ultraviolet contrast of faculae at wavelength λ.

Aside from the differences compared to the IPCC curve noted in Section 3.2, our time series also differs from cycles $15-18$ reconstructed by Solanki and Fligge (1998; see their Figure 2). These authors used a composite of several Ca K and white light facular proxies, prior to the availability of A_{pn}. However, those active region facular proxies do not provide
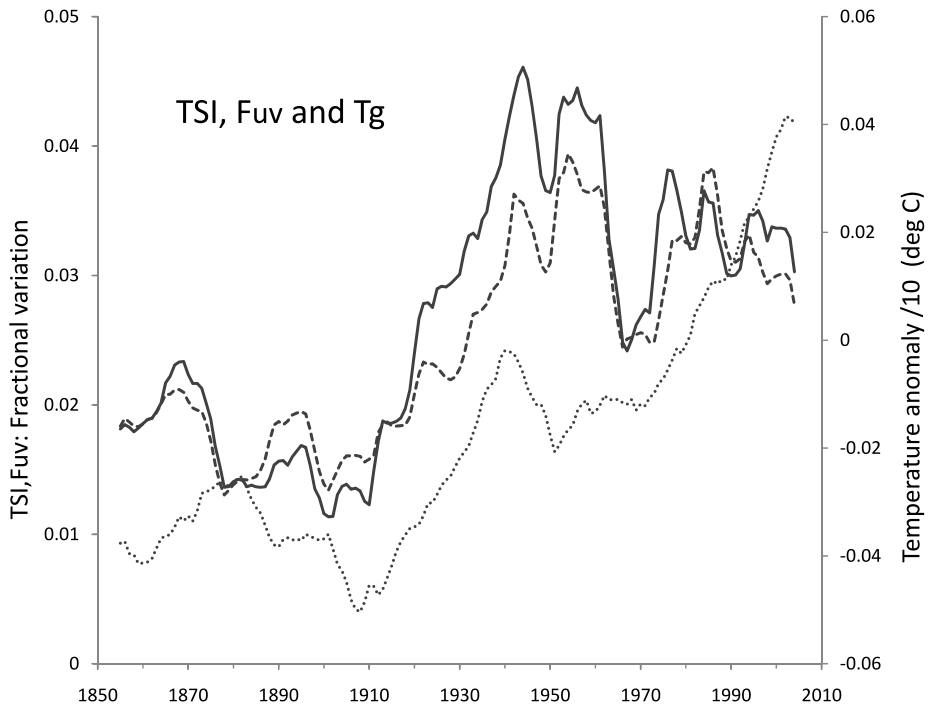
Figure 6 11-yr smoothed time series of: i) TSI (solid), ii) F_{uv} (dashed), iii) T_g (dotted). Ordinates: for (i, ii): fractions of TSI and F_{uv}; for (iii): (degrees C)/10.

a good indicator of the changes in enhanced network that account for TSI variation over the 11-yr cycle.

Our reconstruction of F_{uv} variation between 1610–2009 is shown in Figure 5(b). It is calculated as discussed in Section 2.2 using A_{pn} between 1916–1946, F10.7 between 1947–2009, R_Z between 1875–1916, and R_g prior to 1875. It shows stronger cycles 16 and 17 than the curve given by Lean, Beer, and Bradley (1995; see their Figure 2, panel (b) thin line; active regions only), which is based on R_g in that time period. As for TSI, this difference arises from an increase in the facula/spot area ratio in those cycles. It is interesting that the 11-yr minima of the F_{uv} curve do not exhibit the upward trend seen in TSI, during the early twentieth century. This is because the upward trend in TSI is caused by spot areas that are even lower than usual, rather than by high facular areas, during those minima.

3.5. Comparison of TSI and F_{uv} and Their Correlations with T_g, between 1850–2009

Figure 6 shows the 11-yr smoothed behavior of TSI and F_{uv} after 1850, when direct measurements of global temperature, T_g, became available. The correlation coefficient between the two smoothed time series of TSI and F_{uv} is $r = 0.94$; the main difference is in the reversal in relative amplitudes of the two maxima around 1945 and 1955. The correlation coefficient of T_g with smoothed TSI is $r = 0.66$; it rises to $r = 0.83$ over the shorter period 1850–1970, which excludes the past 40 yr when T_g is widely considered to have been influenced by anthropogenic warming. The corresponding correlations between F_{uv} and T_g are 0.72 and 0.79.

This finding of similar correlations of TSI and F_{uv} with T_g differs from our previous result (Foukal, 2002) for the shorter time period 1916 – 1999. There, the correlation of T_g with F_{uv} was much lower than with TSI. But Figure 6 shows that this correlation arises mainly from the common minimum in all three curves around 1910. This minimum was not included in the shorter data set of our earlier study. The rapid decrease of T_g after 1940 is not seen in the irradiance curves, whose broad maxima extend for about two more decades to approximately 1960.

4. Solar Dimming during the Maunder Minimum

The minima of the 11-yr TSI modulation shown in Figure 5 represent the irradiance received from the quiet Sun. This originates from a photosphere which, even in the absence of active regions, still contains significant magnetic flux in the form of small network and internetwork flux tubes (Harvey, 1977). Their contribution to irradiance is poorly known, since their cross sections extend down to sizes below the resolution limit of even the most powerful solar telescopes.

Kilogauss-intensity flux tubes brighten the Sun through formation of photospheric cavities that facilitate the escape of radiation (Spruit, 1976). Weaker fields are not expected to form effective cavities since their depth depends upon the square of the field intensity (Schnerr and Spruit, 2011). This is an important constraint on proposed connections between changes in quiet, open solar fields, and TSI. The additional solar dimming that could occur if the intense flux tubes entirely disappeared during an extended activity hiatus such as the seventeenth century Maunder Minimum (Eddy, 1976) has been estimated to be roughly 0.1 – 0.2 % (Lean, Skumanich, and White, 1992). This agrees with more direct photometric measurements (Foukal, Ortiz, and Schnerr, 2011; Schnerr and Spruit, 2011), but so far these have been carried out only in two narrow passbands at 630.2 nm and 676.8 nm. Broader band measurements are planned to better approximate the TSI effect.

The extent of the network's disappearance during the seventeenth century is also uncertain. Schrijver *et al.* (2011) argue against such a disappearance, mainly from their finding that the 12-month smoothed, full disk, solar Ca K flux is not significantly lower around 2009 than in the previous activity minima around 1986 and 1996. But closer inspection of their data (see their Figure 2) shows that the individual Ca K observations in 2009 do cluster at slightly lower flux values than in the previous minima.

Certainly, the anomalously low values of other facular indices during the 2009 minimum argue against the conclusion of Schrijver *et al.* (2011) (and also that of Judge and Saar, 2007) that the network could not decay below its 2009 state. The length of the 2008 – 2009 minimum exceeded that of normal minima by only about 1 yr, yet in 2009 the most reliable activity indices like F10.7 and Mg II had already dropped by ≈ 5 % below their normal minimum values (Fröhlich, 2009). It seems unlikely that these indices would not decrease even more if the minimum state lasted for about 70 yr, as during the seventeenth century.

Recent results from solar photometry indicate that the TSI effectiveness of photospheric faculae increases with decreasing cross section (Foukal, Ortiz, and Schnerr, 2011). That is, as solar activity decreases, the TSI decrease caused by removal of the smallest remaining faculae is greater than expected from modeling of the 11-yr TSI modulation by active regions. This finding makes it *more likely* that seventeenth century solar dimming was greater than the 0.02 % lower limit due to disappearance of active regions, but it does not prove that it took place.

However, chromospheric proxies do seem to scale linearly with magnetic flux and therefore with facular size (Skumanich, Smythe, and Frazier, 1975), so we expect to find TSI

decreases below normal quiet Sun values to be accompanied by proportionately smaller *fractional* decreases in chromospheric indices. This is consistent with the findings (Foukal, Bernasconi, and Fröhlich, 2009; Fröhlich, 2009) that the anomalous decrease of the F10.7 and Mg II chromospheric indices in 2008 by about 5 % of their solar cycle range was about four to five times smaller than the fractional TSI decrease. This anomalous TSI decrease is seen in the low 2008 – 2009 PMOD TSI values shown in Figure 5(a).

The greater TSI effectiveness also suggests that TSI might have decreased by enough to influence climate without necessarily removing all photospheric magnetism. This is important because radioisotope studies of [10]Be (*e.g.*, Beer, Tobias, and Weiss, 1998) indicate a weakened 11-yr cycle persisting through the Maunder Minimum. More generally, the [10]Be evidence can provide information on the heliospheric magnetic field and on the open solar field. Steinhilber, Beer, and Fröhlich (2009) have used an empirical relation between measured TSI and open solar magnetic flux at the past three activity minima (Fröhlich, 2009) to estimate a 0.04 % lowering of TSI during the Maunder Minimum. They point out that this small lowering would still have only a modest effect on climate.

A much larger (0.5 %) TSI lowering between the present and the Maunder Minimum is claimed by Shapiro *et al.* (2011), who also used [10]Be, but connected its variation to irradiance through an assumed relation between solar magnetic field energy and irradiance variation. As shown in Section 5 below, their model can be ruled out by comparing its predictions for the twentieth century with observations of the photospheric magnetic network.

In a different approach, a 0.1 % secular brightening between the Maunder Minimum and the 1950s has been ascribed by Tapping *et al.* (2007) to changes in subphotospheric field effects on convection, and thus on the photospheric effective temperature. Their treatment overlooks the powerful damping of any subphotospherically generated TSI variations by the enormous thermal inertia of the convection zone (see, *e.g.*, reviews by Spruit, 1994; Foukal *et al.*, 2006). Given the roughly 2×10^5 yr radiative relaxation of the convection zone, a 0.1 % variation on centennial time scales implies huge (≈ 10 %) variations in heat flux at significant depth, where Tapping *et al.* (2007) propose their luminosity variations originate.

5. Evidence Against Rapid Solar Brightening during the First Half of the Twentieth Century

The model of Lean, Skumanich, and White (1992) predicted, aside from additional dimming during the Maunder Minimum, also a continuing, 0.1 % rise in the zero level of TSI *during the first several activity minima* of the twentieth century. The authors ascribed this brightening to an increase in area of the photospheric magnetic network. But such a 0.1 % brightening during the first half of the twentieth century would have required the *complete disappearance* of the magnetic network going back in time to 1900 (Foukal and Milano, 2001). Such a disappearance is contradicted by clear images of the Ca K network at Mt. Wilson and Meudon Observatories, extending back to the network's discovery in the 1890s by G. Hale and H. Deslandres. Contrary to the claims of Solanki and Krivova (2004), this test is unaffected by uncertainties in Ca K spectroheliogram calibration.

Shapiro *et al.* (2011) find a much larger brightening of about 4 W m^{-2} (or about 0.3 %) between activity minima from 1900 to 1950. They attribute the brightening specifically to small-scale magnetic fields produced by turbulent cascades in the network and intranetwork. However, this brightening is roughly *twice* the estimated 0.1 – 0.2 % contribution of the quiet network to TSI noted above. This obvious contradiction raises serious questions about the Shapiro *et al.* model's underlying assumptions and its applicability to climate forcing in any epoch.

    The reconstruction of Steinhilber, Beer, and Fröhlich (2009), on the other hand, predicts only a very small (≈ 0.01 %) increase in TSI between activity minima during the twentieth century. Such a small change could be produced by a few percent change in network area falling within the 0.007 % yr^{-1} rms detection threshold of the null slope found in the Foukal and Milano (2001) measurements. The same may be true of the small upward trend in open field between 1900–1950 inferred from the heliomagnetic aa index by Svalgaard and Cliver (2010). Their recent review of the data does not support earlier claims for a doubling of the open field and a large TSI uptrend in the twentieth century (Lockwood, Stamper, and Wild, 1999).

6. Conclusions

 i)   Our reconstruction of TSI from direct measurements of facular area produces values 30–50 % higher during cycles 16 and 17 than those currently used by the IPCC for climate studies during the rapid global warming of the early twentieth century. The IPCC values are taken from the reconstructions by Wang, Lean, and Sheeley (2005) which are based on sunspot group number, a less direct proxy of facular area. The difference between TSI (A_{pn}) and the IPCC TSI values arises from an increased ratio of facular areas to spot areas in these cycles (Brown and Evans, 1980; Foukal, 1998b). Such cycle-to-cycle changes in this ratio are an interesting property of subphotospheric dynamo behavior (Foukal, 1998a). These changes are *not* a consequence of carryover of facular fields between cycles, as represented in models of field transport by diffusion (Wang, Lean, and Sheeley, 2005) or by parameterized lifetimes (Solanki, Schüssler, and Fligge, 2002).

 ii) The broad, mid-twentieth century irradiance peak we find extends to about 1960, thus roughly 20 yr beyond the onset of climate cooling after 1940. The correction to post-WWII sea surface temperature measurements reported by Thompson *et al.* (2008) reduces but does not remove this contrasting behavior of irradiance and T_{g}. This failure of correlation, together with the low TSI variation amplitude, casts doubt on a significant role of TSI variation in twentieth century global warming. Driving by F_{uv} is even less likely, since the "top-down" mechanism (Haigh, 1996; Shindell *et al.*, 2006) seems to affect storm tracks and precipitation more clearly than it affects T_{g}. Thus, the UV driving mechanism is also unlikely to provide the connection sought between solar activity and global temperature over centennial or longer time scales, unless additional couplings are considered (*e.g.*, Meehl *et al.*, 2009).

 iii) Recent findings from photospheric imaging indicate that the emergent radiative flux/area from a facula increases with decreasing size (Foukal, Ortiz, and Schnerr, 2011). Removal of faculae of decreasing size as the Sun becomes more quiet during *extended* activity minima might then decrease TSI (but not F_{uv}) more than expected from previous linear models. The ^{10}Be evidence for decrease in open solar field and TSI during the Maunder Minimum reported by Steinhilber, Beer, and Fröhlich (2009) is more consistent with such flux tube removal than with variations in solar effective temperature attributed to sub photospheric convective changes (Tapping *et al.*, 2007; Fröhlich, 2009). Any deep-lying heat flux variations would be heavily damped by the thermal inertia of the solar convection zone.

 iv) Arguments for a sharp TSI rise in the first half of the twentieth century (*e.g.*, Shapiro *et al.*, 2011) require *complete disappearance* of the photospheric magnetic network going back in time from the 1950s toward 1900. Such a disappearance is contradicted by the

presence of a fully developed network in Ca K spectroheliograms obtained at Mt. Wilson and Meudon Observatories since the 1890s. This casts serious doubt on the basic model of Shapiro *et al.* and its claims for strong irradiance forcing through the Holocene.

Appendix: Accuracy of the Ca K Facular Area Measurements

The accuracy of the A_p and A_{pn} facular indices has been questioned by Ermolli *et al.* (2009), on the grounds that the area measurements were made from photographic density, rather
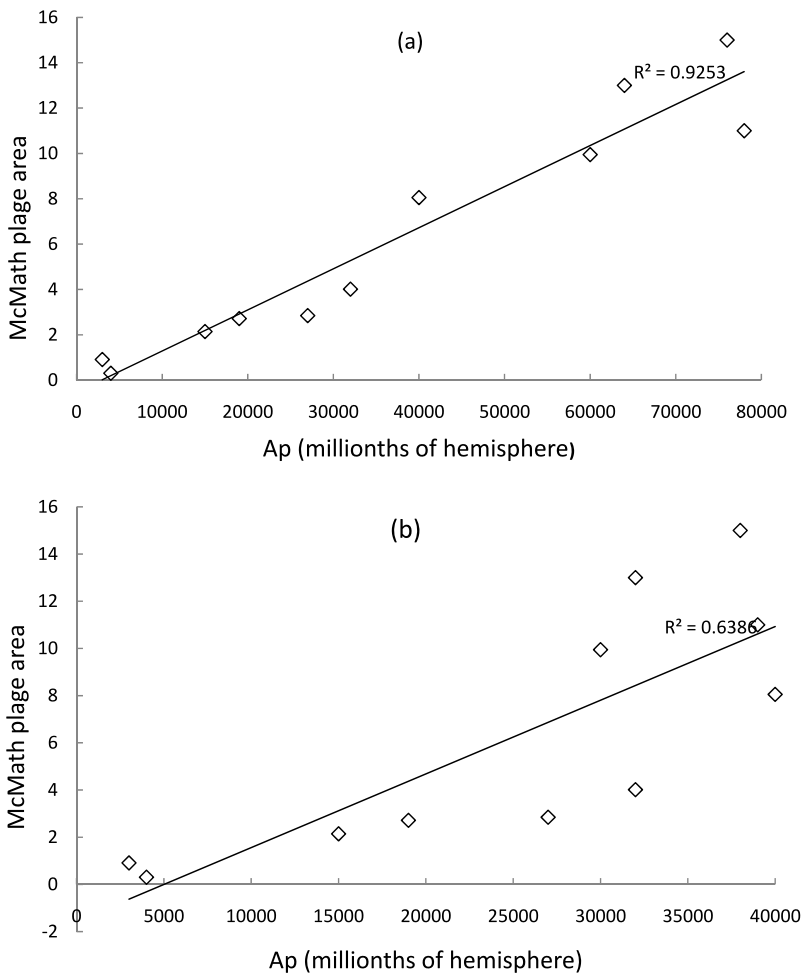

Figure 7   Panel (a): McMath–Hulbert plage areas (millionths of a hemisphere) for cycle 19 (ordinate) plotted against A_p. Panel (b): As above, but plotted against A_p with the four highest A_p values replaced by the values proposed by Ermolli *et al.* (2009).
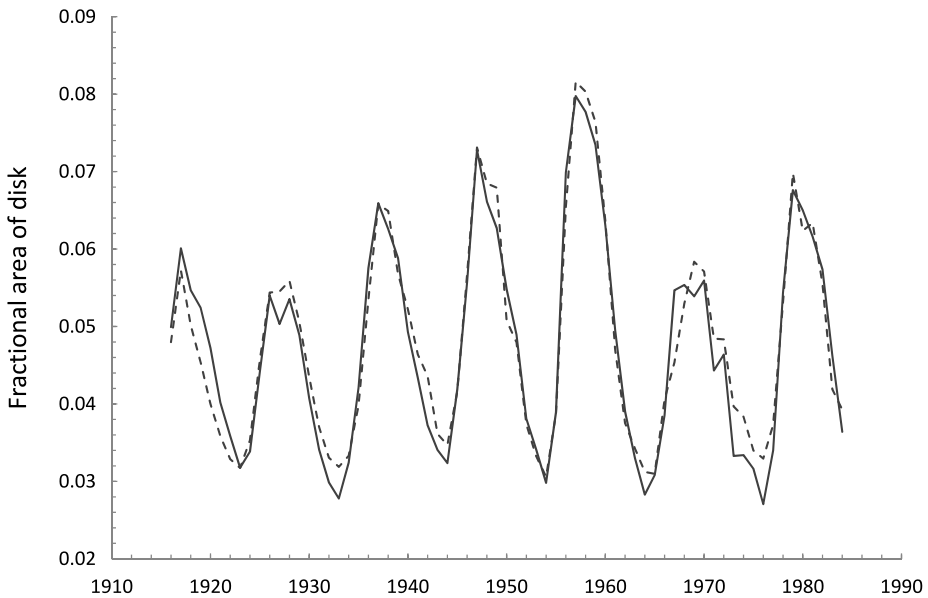
Figure 8 Comparison of the annual mean Ca K facular area indices A_{pn} (solid) and UCLA (dashed). The values of the two time series have been normalized.

than from calibrated relative intensity. Here A_p measures areas (corrected for projection) of active region faculae, whereas the A_{pn} also includes the active network (projected) areas.

Regarding A_p, they report that, while their photographically calibrated reduction of the MWO data generally agrees with the A_p index to within 10 % over the 1915 – 1984 period, it disagrees by a factor two on the four years of highest activity in cycle 19. In Figure 7 we compare annual mean A_p with the McMath–Hulbert plage index, widely used between 1954 – 1987. This index (Swartz and Overbeck, 1971) measures the area of active region plages (like A_p, not including enhanced network) weighted by a rough eye-estimate of plage relative intensity.

We see that the correlation of A_p with this independent McMath index during cycle 19 yields $r^2 \approx 0.92$. The discrepancy between A_p and the Ermolli *et al.* (2009) data for those four years (see Figure 8 in Ermolli *et al.*, 2009) does not exist in the comparison of A_p with the McMath index shown in Figure 7. On the contrary, replacing our values with those of Ermolli *et al.* (2009) reduces the correlation to $r^2 = 0.64$. Therefore, it appears that the problem reported by Ermolli *et al.* (2009) lies with their reduction, and not with an error in A_p. The McMath measurements were, like the A_p measurements, based on uncalibrated photographic images. But their independent choices of film, exposures, contrast, and plage boundaries were unlikely to replicate ours.

Regarding A_{pn}, comparison of annual mean A_{pn} with the two independent reductions of the same Mt. Wilson images by teams from UCLA (Bertello, Ulrich, and Boyden, 2010) and from Pulkovo Observatory (Tlatov, Pevtsov, and Singh, 2009) exhibits close agreement (see Figure 8; also Figure 1 in Foukal *et al.*, 2009). The A_{pn} values were measured from un-calibrated densities; the UCLA measurements were carried out from (uncertain) calibrated relative intensities. This shows that separate reductions of the same spectroheliograms us-ing different pixel resolution, photometric resolution and calibrations, and thresholds can produce remarkably similar results.
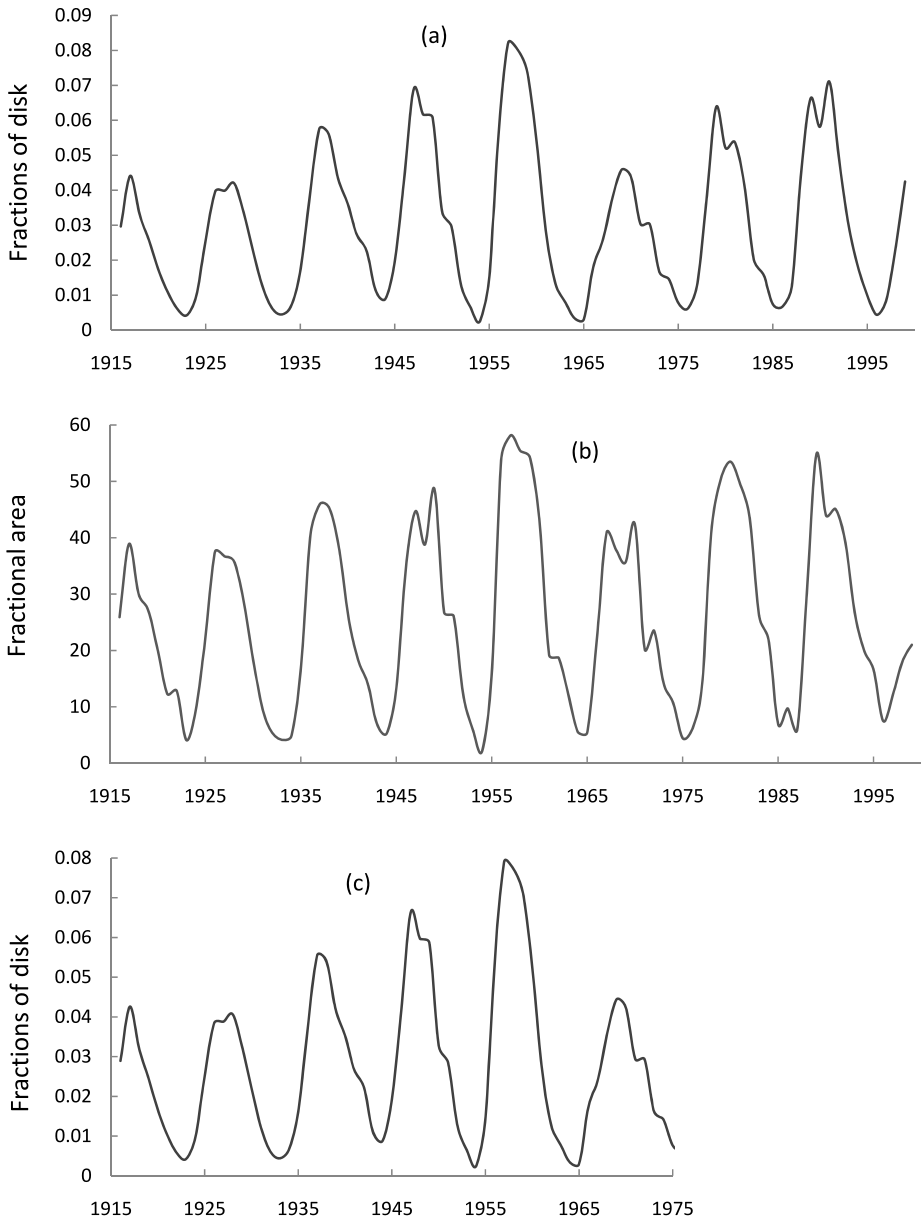
Figure 9   Panel (a): The facular area time series A_{pn} (in fractions of the disk); panel (b): Kodaikanal facular areas (in thousandths of a hemisphere); panel (c): the facular areas corrected for sunspot area, *i.e.*, $(A_{pn} - A_s)$.

Tlatov, Pevtsov, and Singh (2009) and Foukal *et al.* (2009) have shown less satisfactory agreement between separate reductions of the MWO and SPO spectroheliograms on one hand, versus the same time periods using the KKL spectroheliograms. In particular, the amplitudes of cycles 18 and 19 compared to other cycles is much smaller in KKL than in A_{pn} or in the UCLA reduction of the MWO data. Comparison of the relative amplitudes

of cycles 21, 22 between the two separate reductions of the SPO data for 1985–1999 by Tlatov, Pevtsov, and Singh (2009) and by Foukal (2002) also show less good agreement than for the MWO 1915–1984 data.

The KKL (and SPO) data were obtained using a wider spectral passband than the Mt. Wilson data, and as noted by Ermolli *et al.* (2009), sunspots are easier to identify than in the MTW data. In fact, spot areas were included in the plage areas in the A_p and A_{pn} and other MWO-based indices, as well as in the McMath–Hulbert plage index. Tlatov, Pevtsov, and Singh (2009) suggested that this inclusion of spots might explain the difference between the MWO versus the SPO and KKL results.

In Figure 9 we compare the KKL and MWO data with and without a correction for spot area. It can be seen that the spot area contribution to the much larger plage area is only at the 5 % level. Therefore, this cannot be the correct explanation of the MWO versus KKL and SPO differences, which reach 30 %. The reason for this disagreement, and between the independent reductions of the SPO 1985–1999 data, requires further investigation.

References

Beer, J., Tobias, S., Weiss, N.: 1998, *Solar Phys.* **181**, 237.
Bertello, L., Ulrich, R., Boyden, J.: 2010, *Solar Phys.* **264**, 31.
Brown, G., Evans, D.: 1980, *Solar Phys.* **66**, 233.
Camp, C., Tung, K.: 2007, *Geophys. Res. Lett.* **34**, 14703.
Chapman, G., McGuire, T.: 1977, *Astrophys. J.* **217**, 657.
Crowley, T.: 2000, *Science* **289**, 270.
Eddy, J.: 1976, *Science* **192**, 1189.
Ermolli, I., Solanki, S., Tlatov, A., Krivova, N., Ulrich, R., Singh, J.: 2009, *Astrophys. J.* **698**, 1000.
Foukal, P.: 1996, *Geophys. Res. Lett.* **23**, 2169.
Foukal, P.: 1998a, *Astrophys. J.* **500**, 958.
Foukal, P.: 1998b, *Geophys. Res. Lett.* **25**, 2909.
Foukal, P.: 2002, *Geophys. Res. Lett.* **29**, 2089.
Foukal, P., Bernasconi, P., Fröhlich, C.: 2009, *Bull. Am. Astron. Soc.* **41**, 827.
Foukal, P., Bertello, L., Livingston, W., Pevtsov, A., Singh, J., Tlatov, A., Ulrich, R.: 2009, *Solar Phys.* **255**, 229.
Foukal, P., Chulsky, G., Weisenstein, D.: 2008, AGU Spring Meeting SP 53B-06.
Foukal, P., Fröhlich, C., Spruit, H., Wigley, T.: 2006, *Nature* **443**, 161.
Foukal, P., Lean, J.: 1988, *Astrophys. J.* **328**, 347.
Foukal, P., Lean, J.: 1990, *Science* **247**, 505.
Foukal, P., Milano, L.: 2001, *Geophys. Res. Lett.* **28**, 883.
Foukal, P., Ortiz, A., Schnerr, R.: 2011, *Astrophys. J. Lett.* **733**, L38.
Fröhlich, C.: 2009, *Astron. Astrophys.* **501**, L27.
Fröhlich, C.: 2011, *Contrib. Astron. Obs. Skaln. Pleso* **35**, 1.
Harvey, J.: 1977, In: Muller, E. (ed.) *IAU Highlights Astron*, **4**, 223.
Haigh, J., Blackburn, M., Day, R.: 2005, *J. Climate* **18**, 3672.
Haigh, J.: 1996, *Science* **272**, 981.
Hathaway, D., Wilson, R., Reichmann, E.: 2002, *Solar Phys.* **211**, 357.
Hoyt, D., Schatten, K.: 1998, *Solar Phys.* **179**, 189.
Judge, P., Saar, S.: 2007, *Astrophys. J.* **663**, 643.
Kopp, G., Lean, J.: 2011, *Geophys. Res. Lett.* **38**, 01706.
Krivova, N., Solanki, S.: 2008, *Astron. Astrophys.* **29**, 151.
Lean, J.: 1987, *J. Geophys. Res.* **92**, 839.
Lean, J., Beer, J., Bradley, R.: 1995, *Geophys. Res. Lett.* **22**, 3195.
Lean, J., Skumanich, A., White, O.: 1992, *Geophys. Res. Lett.* **19**, 1591.
Lean, J., Wang, Y.-M., Sheeley, N.: 2002, *Geophys. Res. Lett.* **29**, 2224.
Lockwood, M., Stamper, R., Wild, M.: 1999, *Nature* **399**, 437.
Meehl, G., Arblaster, J., Matthes, K., Sassi, F., Van Loon, H.: 2009, *Science* **325**, 1114.
North, G., Wu, Q., Stevens, M.: 2004, In: Pap, J.M., Fox, P., Frohlich, C., Hudson, H.S., Kuhn, J., McCormack, J., North, G., Sprigg, W., Wu, S.T. (eds.) *Solar Variability and Its Effects on Climate*, *AGU Geophys. Monogr.* **141**, 251.

Schnerr, R., Spruit, H.: 2011, *Astron. Astrophys.* **532**, 136.
Schrijver, K., Livingston, W., Woods, T., Mewaldt, R.: 2011, Geophys. Res. Lett. **38**. doi:10.1029/2011GL046658.
Shapiro, A.J., Schmutz, W., Rozanov, E., Schoell, M., Haberreiter, M., Shapiro, A.V., Nyeki, S.: 2011, *Astron. Astrophys.*, **529**, 67.
Shindell, D., Faluvegi, G., Miller, R., Schmidt, G., Hansen, J.: 2006, *Geophys. Res. Lett.* **33**, 24706.
Skumanich, A., Smythe, C., Frazier, E.: 1975, *Astrophys. J.* **200**, 747.
Solanki, S., Fligge, M.: 1998, *Geophys. Res. Lett.* **25**, 341.
Solanki, S., Krivova: 2004, *Solar Phys.* **224**, 197.
Solanki, S., Schüssler, M., Fligge, M.: 2002, *Astron. Astrophys.* **383**, 706.
Solomon, S., Qin, D., Manning, M., Chen, Z., Marquis, B., Averyt, T., Tignor, M., Miller, H. (eds.): 2007, *Working Group I Contribution to Fourth IPCC Assessment Report*, Cambridge Univ. Press, Cambridge.
Spruit, H.: 1976, *Solar Phys.* **50**, 269.
Spruit, H.: 1994, In: Pap, J. (ed.) *The Sun as a Variable Star: Solar and Stellar Irradiance Variations*, *IAU Colloq.* **142**, 270.
Steinhilber, F., Beer, J., Fröhlich, C.: 2009, *Geophys. Res. Lett.* **36**, 19704.
Svalgaard, L., Bertello, L.: 2009, *Bull. Am. Astron. Soc.* **41**, 837, Abstract 15:13.
Svalgaard, L., Cliver, E.: 2010, *J. Geophys. Res.* **115**, AO9111.
Swartz, W., Overbeck, R.: 1971, *Penn State Univ. Scientific Report* **373**.
Tapping, K.: 1987, *J. Geophys. Res.* **92**, 89.
Tapping, K., Boteler, D., Charbonneau, P., Crouch, A., Manson, A., Paquette, H.: 2007, *Solar Phys.* **246**, 309.
Thompson, M., Kennedy, J., Wallace, J., Jones, P.: 2008, *Nature* **453**, 646.
Tlatov, A., Pevtsov, A., Singh, J.: 2009, *Solar Phys.* **255**, 239.
Wang, Y.-M., Lean, J., Sheeley, N.: 2005, *Astrophys. J.* **625**, 522.
Wang, Y.-M., Nash, A., Sheeley, N.: 1989, *Science* **245**, 712.
Wigley, T., Raper, S.: 1990, *Geophys. Res. Lett.* **17**, 2169.
Willson, R., Gulkis, S., Janssen, M., Hudson, H.: 1981, *Science* **211**, 700.